



INTERNATIONAL ATOMIC ENERGY AGENCY
UNITED NATIONS EDUCATIONAL, SCIENTIFIC AND CULTURAL ORGANIZATION
INTERNATIONAL CENTRE FOR THEORETICAL PHYSICS
I.C.T.P., P.O. BOX 586, 34100 TRIESTE, ITALY, CABLE: CENTRATOM TRIESTE



SMR.703 - 10

**WORKING PARTY ON
MECHANICAL PROPERTIES OF INTERFACES**

23 AUGUST - 3 SEPTEMBER 1993

"Fractal Description of Intergranular Fractures"

**Chi-Wei LUNG
Institute of Metal Research
Academia Sinica
Wenhua Road 72
Shenyang 110015
People's Republic of China**

These are preliminary lecture notes, intended only for distribution to participants.

MAIN BUILDING STRADA COSTIERA, 11 TEL. 22401 TELEFAX 224163 TELEX 460392 ADRIATICO GUEST HOUSE VIA GRIGNANO, 9 TEL. 224241 TELEFAX 224531 TELEX 460449
MICROPROCESSOR LAB. VIA BEIRUT, 31 TEL. 224471 TELEFAX 224163 TELEX 460392 GALILEO GUEST HOUSE VIA BEIRUT, 7 TEL. 22401 TELEFAX 224559 TELEX 460392

FRACTALS AND THE FRACTURE OF CRACKED METALS

C.W. LUNG

International Centre for Theoretical Physics, Trieste, Italy and Institute of Metal Research, Academia Sinica, Shenyang, People's Republic of China *

A fractal model for intergranular brittle and ductile fracture surfaces of cracked metals is suggested. It is shown that for small grain size metals, the critical crack extension-force would rise rapidly and faster than the Hall-Petch's relationship due to the increase of the true areas of the irregular fracture surfaces.

1. INTRODUCTION

The fracture surface formed after breaking off is rough and irregular. Mandelbrot et al^{1,2} showed that the structure of fracture surfaces of metals was modelled very well by a fractal surface, though metal fractures are only extremely crinkly (down to the limits of their microstructural size range), while fractals are infinitely crinkly. Their experiments in metal fracture showed that the fractal dimension D was very well defined for different specimens of the same metal having similar thermomechanical treatments.

We think that the sizes and orientations of grains in many polycrystalline metals are "irregular" (the distribution of impurities, defects and other internal stress sources are also "irregular"). These may be the physical foundation for many metal fracture surfaces being successfully modelled by fractals.

In this paper, we analyze the grain size effects on the fracture of metals with fractal models.

2. THE CRITICAL CRACK EXTENSION FORCE

On the Griffith theory for perfectly elastic fractures³, it would have to exceed the work needed to separate the two surfaces, $2\gamma_s$. In

Irwin's approach in fracture mechanics, the critical strain energy release rate, i.e. the critical crack extension force, G_{crit} ³ may be written as

$$G_{crit.} = 2\gamma_s \quad (\text{for brittle fracture}) \quad (1)$$

$$\text{and} \quad G_{crit.} = 2\gamma_s + \gamma_p \quad (\text{for quasi-brittle fracture}) \quad (2)$$

where γ_p represents the energy expended in the plastic work necessary to produce unstable crack propagation at the crack tip.

Unlike in glass, the fracture surfaces in metals are rough and irregular. The true areas of the fracture surfaces in metals are actually larger than the data got by macroscopic measurements. The area of the fracture surface per unit thickness of specimen would be $[L(\epsilon)/L_0(\epsilon)] \cdot 1$ (in fracture mechanics, we always simplify the crack as a line in a two-dimensional system). Then, instead of Eq.(1) and Eq.(2), we have (Fig.1a,b).

$$G_{crit.} = 2(L(\epsilon)/L_0(\epsilon))\gamma_s \quad (3)$$

and

$$G_{crit.} = 2(w-a)^{-1}[L_1(\epsilon_1) + L_2(\epsilon_2)]\gamma_s + \gamma_p \quad (4)$$

where ϵ_i 's are the yardstick lengths. Other parameters have been shown in Figs.1.

* Permanent address.

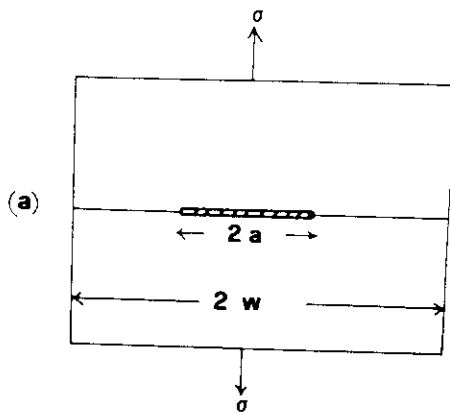


FIGURE 1a

Ideal brittle fracture in glass.

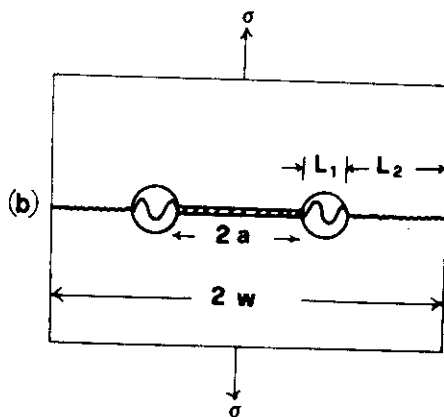


FIGURE 1b

Elastic plastic fracture in metal.

3. A FRACTAL MODEL FOR INTERGRANULAR BRITTLE FRACTURE SURFACES OF METALS

In the intergranular fracture case, the crack would propagate along zigzag grain boundaries. In a smaller scale, the crack would propagate along smaller zigzag subgrain boundaries. In a larger scale, the crack would also propagate along a larger weak passage near by the general direction of crack propagation and which would be formed by irregular distributions of vacancy clusters, micro-voids, inclusions and micro-

cracks etc. They are all irregular and can be considered as self-similar and then can be modelled by fractals (Fig.2). In addition, I believe that the fractal dimension D might be well defined for different specimens of the same metal not only having similar thermomechanical treatments¹ but also under the same temperature condition and loading rate of the tensile test.

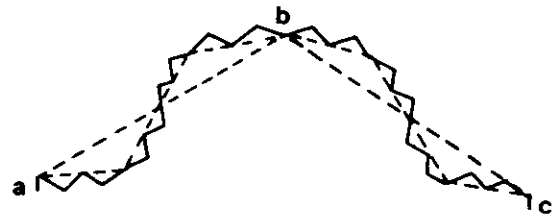


FIGURE 2

New refined zigzag cracks formed in fractal modelled metals.

There are two forms of intergranular brittle fracture (Figs.3a and b). Their fractal dimensions can be estimated by the formal definition

$$D = \log N / \log \left(\frac{1}{r} \right), \quad (5)$$

where $N = L_1 / \epsilon_{01}$, $r = \epsilon_{01} / L_{01}$ (Figs.3).

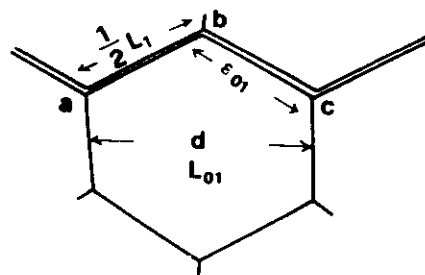


FIGURE 3a

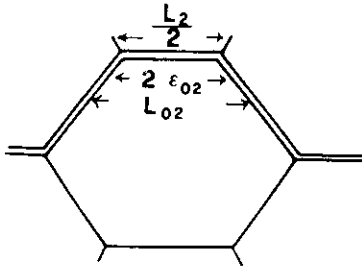


FIGURE 3b

Intergranular brittle fracture.

$$(a) \quad N = 2, \quad r = \frac{1}{1.732}, \quad D = 1.26,$$

$$(b) \quad N = 4, \quad r = \frac{1}{3}, \quad D = 1.26.$$

Both fractal dimensions of the two forms are 1.26, but the grain sizes are different. The grain size, d ,

$$d = L_{01} = 1.73 \epsilon_{01} = 3.46 \epsilon_{02}, \quad (6)$$

where $L_1 = 2 \epsilon_{01}$, $L_{01} = 1.73 \epsilon_{01}$, $L_2 = 4 \epsilon_{02}$, $L_{02} = 3 \epsilon_{02}$. From Eq.(3),

$$G_{crit} = 2\gamma_s [L_i/L_{0i}] = 2\gamma_s (L_{0i}/\epsilon_{0i})^{D-1} \quad (7)$$

$$(a) \quad G_{crit} = 1.73^{0.26} \times 2\gamma_s$$

$$(b) \quad G_{crit} = 3^{0.26} \times 2\gamma_s$$

We may see that case (a) consumes less energy than case (b), then it is preferable. The fractal model in this paper is then based on case (a).

As the grain size is smaller and smaller, the true area of fracture surface becomes larger and larger. According to Mandelbrot²,

$$L_i(\epsilon_i) \sim F \epsilon_i^{1-D} \quad (F = L_0^D) \quad (8)$$

$$G_{crit} = 2\gamma_s (L_i/L_0) \approx 2\gamma_s F L_0^{-1} \epsilon_i^{1-D} \approx 2\gamma_s d^{-0.26} (1.73^{0.26} \approx 1.1)$$

($F L_0^{-1} = L_0^{D-1} = 1$, for choosing L_0 as a unit length, say 1 cm). Then,

$$G_{crit} = 2\gamma_s \times 10.96 \quad (\text{for } d = 10^{-4} \text{ cm})$$

$$G_{crit} = 2\gamma_s \times 20 \quad (\text{for } d = 10^{-5} \text{ cm})$$

$$G_{crit} = 2\gamma_s \times 36.3 \quad (\text{for } d = 10^{-6} \text{ cm})$$

The term related to γ_s in Eq.(2) is now comparable to or a little smaller than the term related to γ_p (usually $\gamma_p \gg 10\gamma_s$) in brittle fracture; but, it is still not large enough to improve the fracture toughness of materials. However, it might be one of the reasons why the surface energies of metals estimated by low temperature brittle fracture measurements are always higher than by other methods.

4. A FRACTAL MODEL FOR THE INTERGRANULAR DUCTILE FRACTURE SURFACES OF METALS

The fractographic observations on intergranular fracture indicate that the ductile fracture surface is composed of microdimples which are the result of holes forming ahead of the main crack. These holes are thought to initiate in practical alloy steels primarily at the site of precipitated particles in the matrix. Often the large voids in the medium are connected by bands of intense shear, which are formed by dislocation motions. As to our simplified fractal model, plastic deformations in the grains would make the grain boundaries ab and bc to be curves, ab' and $b'c$. Moreover, ab' and $b'c$ are steeper than ab and bc . An additional angle θ would appear (Fig.4) after loading



FIGURE 4

The additional angle formed by plastic deformation in the grain.

Now,

$$L^P = 2\epsilon$$

$$L_0 = 2\epsilon \cos(30^\circ + \theta) \quad .$$

In this case, $N = 2$, $r = [2 \cos(30^\circ + \theta)]^{-1}$

$$D = \log 2 / \log [2 \cos(30^\circ + \theta)] \quad (9)$$

The value of θ can be estimated as follows

$$\theta = (\rho b L) / L = \rho b \quad , \quad (10)$$

where ρ is the linear density of mobile dislocations. Typical values of total linear density of dislocations range from 10^6 - 10^7 /cm for cold worked crystals to 10^3 /cm for annealed crystals. With $b \approx 3 \times 10^{-8}$ cm, the range of θ in Eq.(10) is from 3×10^{-5} (rad.) to $0.03 - 0.3$ (rad.) ($1.7^\circ - 17^\circ$). Then, the fractal dimensions range from 1.26 to 2.23.

Taking $D = 2.23$; then,

$$G_{\text{crit}} \approx 2\gamma_s d^{-1.23}$$

$$G_{\text{crit}} = 2\gamma_s \times 8.3 \times 10^4 \quad (\text{for } d = 10^{-4} \text{ cm})$$

$$G_{\text{crit}} = 2\gamma_s \times 1.4 \times 10^6 \quad (\text{for } d = 10^{-5} \text{ cm})$$

The critical crack extension force estimated by this fractal model would rise rapidly with the decrease of grain size. It rises faster than the Hall-Petch's $d^{-1/2}$ law, if the density of mobile dislocation is high enough. We noted

that the grain sizes of almost of the superplastic alloys are very small ($< 10^{-4}$ cm). This phenomenon probably could be explained by this fractal model.

ACKNOWLEDGMENTS

The author would like to thank Professor Abdus Salam, the International Atomic Energy Agency and UNESCO for hospitality at the International Centre for Theoretical Physics, Trieste, where this work was finished during his stay in the summer of 1985. He would also like to thank Professors S. Lundqvist and B.B. Mandelbrot for their helpful discussions. This work is supported by the Science Fund of the Chinese Academy of Science.

REFERENCES

1. B.B. Mandelbrot, D.E. Passoja and A.J. Paullay, *Nature*, Vol.308, 19 (1984) 721.
2. B.B. Mandelbrot, *The Fractal Geometry of Nature* (1983) pp.25, 29, 459.
3. J.F. Knott, *Fundamentals of Fracture Mechanics* (Butterworths, 1976) pp.109-111.
4. C.W. Lung and H. Gao, *Phys. Stat.Sol.(a)*, 87 (1985) 565.

FRACTAL DESCRIPTION OF FRACTURES

C.W. Lung

International Centre for Theoretical Physics, Trieste, Italy
and
International Centre for Mat. Physics, Institute of Metal Research
Academia Sinica, 110 015 Shenyang, PR of China

ABSTRACT

Recent studies on the fractal description of fractures are reviewed. Some problems on this subject are discussed. It seems hopeful to use the fractal dimension as a parameter for quantitative fractography and to apply fractal structures to the development of high toughness materials.

I. INTRODUCTION

In 1984, Mandelbrot *et al.* [1] showed that fractured surfaces are fractals in nature and that the fractal dimensions of the surfaces correlate well with the toughness of the material. Later on, the present author [2] analyzed the critical crack extension force with the fractal model and pointed out that the true areas of the fractured surfaces in materials are actually larger than those indicated by the data obtained by macroscopic measurements. The effective critical crack extension force would thereby be larger than that calculated from a flat fractured surface. Herrmann [3] modelled fractures on a square lattice and found that the patterns of cracks can be fractal even without including noise due only to the interplay of anisotropy and memory. The shapes of the cracks can be compared to the ones found experimentally for stress corrosion. Fractal description of fractures is a question of technological importance and also an interesting theoretical problem.

The aim of the present paper is to discuss the problems in recent studies on this subject and to show the possibility of applications of fractals to fractures in materials.

II. FRACTALS IN MATERIALS

A fractal is a shape made of parts similar to the whole in some way [4]. This property, called self-similarity or self-affinity under a scale transformation, is common to all fractal objects. The mathematical fractal model has an infinite number of generations without upper and lower limits; otherwise coarse graining of the initiator or fine graining of the lowest limit of generation would not give the same shape as the original one. Fractals in nature are approximate models. The difference between fractals in nature and rigorous ones are [5, 6]:

1. The range of length in which self-similarity holds is bounded from above by the size of the object and from below of the size of the smallest building block.
2. They usually appear random, but are self-similar in a statistical sense.

Fractals in materials are more complicated and sometimes not so typical as the sea shore, snow flowers and trees even in a statistical sense.

The range of length in which self-similarity holds is small. Some authors pointed out that a constant value of fractal dimension in a certain range of scale is a necessary prerequisite for self-similarity of a structure; e.g. the number of generations should be larger than three and the range of scale should be observable for more than one order of magnitude [7].

The approximation to self-similarity in materials is poor even in a statistical sense. There may be many physical sources of self-similarities in some ranges of scale (Fig.1). The problem is how to find out the main one corresponding to the property you studied.

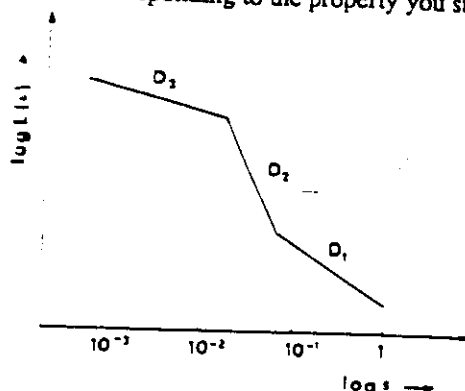


Fig.1 $\log L(\varepsilon) - \log \varepsilon$ plot to determine fractal dimension D_F of a line.

Recently, fractal analysis has been well known and able to apply to structural elements in materials which are usually described by their integer Euclidean dimension, for example, macroscopic crack lines, or planes, vacancies, dislocations, grain boundaries, dispersoid particles etc. However, a fractal structure must be geometrically scaling.

Self-similarity implies that a similar morphology appears in a wide range of magnification in the analysis. Fractured surfaces require careful metallographic analysis to determine not only a D_F value but also to establish their self-similarity. How wide should be the range is an open problem. For instance, the total length, $L_n(\eta)$ of a Koch curve is given by

$$\frac{L_n(\eta)}{L_0(\eta)} = L(\varepsilon) = \varepsilon^{1-D_F} = \left(\frac{\eta}{L_0}\right)^{1-D_F}, \quad L_n(\eta) = L_0 \quad (1)$$

where η is the yardstick length, ε is the normalized yardstick length with respect to L_0 , the length of the initiator ($\varepsilon = \eta/L_0$) and D_F is the fractal dimension of the Koch curve. $\varepsilon = r^n$, r is the reduction in scale by one iteration n .

If $r = \frac{1}{3}$, $n = 2$; then $\varepsilon = \frac{1}{9} \approx \frac{1}{10}$. Two generations are enough to appear the self-similarity in a range of one order of magnitude. However, two generations are not enough to be considered as a fractal at least for measuring the fractal dimension with the slit-island method obviously [8, 9].

Usually, n and r take discrete values; then, from equation 1, the length of the yardstick line cannot change continuously. The measured $\log L_0(\eta) - \log \eta$ plot would be wavy rather than a straight line if you change the yardstick length continuously.

III. THE RELATIONSHIP BETWEEN FRACTAL DIMENSION AND FRACTURE TOUGHNESS OF FRACTURED SURFACES

Unlike previous empirical relations, a model based on linear fracture mechanics theory was proposed [2].

In Irwin's approach in fracture mechanics, the critical strain energy release rate, i.e., the critical crack extension force, G_{1c} may be written as

$$\begin{aligned} G_{1c} &= 2\gamma_s & (\text{for brittle fracture}) \\ G_{1c} &= 2\gamma_s + \gamma_p \sim \gamma_p & (\text{for quasi-brittle fracture}) \end{aligned} \quad (2)$$

where γ_s is the specific surface energy and γ_p represents the energy expended in the plastic work necessary to produce unstable crack propagation at the crack tip. In the quasi-brittle case (or the small scale yielding case) we assume that the plastic zone at the crack tip is very small and the thickness of plastic deformation is very thin.

Owing to the crack propagation along a zigzag line, the true areas of fractured surfaces (or lengths of lines) are actually larger than the data obtained by macroscopic measurements. The area of the fractured surface per unit thickness of specimen would be $[L_n(\eta)/L_0(\eta)] \cdot 1$ (in fracture mechanics, we always simplify the crack as a line in a two-dimensional system). Then, instead of equation 2, we have

$$G_{1c} = 2\gamma_s (L_n(\eta)/L_0(\eta)) \quad (3)$$

and

$$G_{1c} \approx 2\gamma_p (L_n(\eta)/L_0(\eta))$$

From equations 1 and 3, we obtain [2, 8]

$$G_{1c} = (G_{1c})_0 (\eta/L_0)^{1-D_F} \quad (4)$$

and

$$\log G_{1c} = \log (G_{1c})_0 + (1 - D_F) \log (\eta/L_0) \quad (5)$$

The logarithm value of critical crack extension force or fracture toughness is linear in relationship with the fractal dimension of fractured surface (Fig. 2). This relation, based on fracture mechanism, holds in many experimental measurements [8, 10, 11, 12, 13].

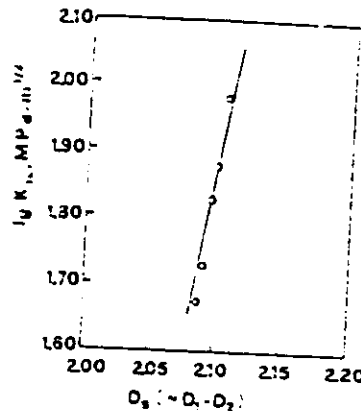


Fig. 2 $\lg K_{Ic}$ vs fractal dimensions $D_s \sim (D_1 + D_2)$.

Furthermore,

$$\frac{\partial(\log G_{1c})}{\partial D_F} = -\log(\eta/L_0) > 0 \quad (6)$$

due to $\eta < L_0$.

Taking care of the scaling range of the fractal, the relation has been derived again recently by Tzschichholz and Pfaff [20].

IV. THE PROBLEM ON THE CORRELATION BETWEEN THE FRACTAL DIMENSION AND THE TOUGHNESS OF MATERIALS

In previous papers [2, 8] (or equation 5 and equation 6), the present author showed that the critical crack extension force, or the fracture toughness increases with the increase of fractal dimension of fractured surface; i.e. the correlation between fractal dimension and fracture toughness is a positive one. Recent experimental data verified this conclusion again [20]. However, some experimental data showed that the correlation between D_F and toughness (dynamic tear energy, fracture toughness etc.) is a negative one [1, 10, 13, 14]. If a high fractal dimension is supposed to be characteristic of a rough surface as opposed to a smooth one, we would conclude that the rough surfaces are to be associated with brittle materials. This is contrary to experiences! This, however, is difficult to explain.

In Section V, I am going to show that the origin of the negative correlation mainly lies in the slit-island method for fractal dimension measurement and in some possible physical sources of crack propagation.

V. DIFFICULTIES OF THE SLIT-ISLAND METHOD

The slit-island method was proposed [1] and was widely used for fractal dimension measurements [10, 14-19]. In spite of various explanations on the dependences of toughness on fractal dimensions [2, 8, 9], Lung and Mu [8], based on experiments, pointed out that the fractal dimension determined by the slit-island method is dependent on the yardstick chosen. The measured value would not be the real fractal dimension of fractured surfaces.

The theoretical base of the slit-island method is that the ratio

$$\alpha_D(\varepsilon) = [L(\varepsilon)]^{1/D_F} / [A(\varepsilon)]^{1/2} \quad (7)$$

is size independent provided ε is constant. However, in practical measurements, we can only keep η constant. We cannot keep $\varepsilon (= \eta/L_0)$ constant due to different sizes of the Koch islands (L_0).

For the Koch perimeter,

$$L_n(\eta) = L_0^{D_F}(\eta) \eta^{1-D_F}$$

the ratio

$$\alpha_n(\eta) = \frac{L_n(\eta)^{1/D_F}}{A_n(\eta)^{1/2}} = L_0(\eta) \eta^{(1-D_F)/D_F} A_n(\eta)^{-1/2} \quad (8)$$

In general, $\alpha_n(\eta)$ is dependent on the size of Koch island (L_0). We cannot obtain a linear relationship between logarithm values of A_n 's and L_n 's of different size similar Koch islands with a constant yardstick length η .

Furthermore, $\varepsilon_i = \eta/L_{0i}$. For the larger island, ε_i is smaller and the smaller normalized yardstick sees more generations. In addition, $\alpha_n(\varepsilon)$ is yardstick dependent, $\alpha_i(\varepsilon_i) \neq \alpha_j(\varepsilon_j)$. The measured values of D_m must be yardstick dependent. As was expected, our experimental data verified the above conclusion (Fig.3) [8]. This would then be one of the origins of the negative correlations between measured D_m and the toughness of materials. Indeed, we changed the yardstick length, a positive correlation between D_m and $G_{1c}(K_{1c})$ was obtained (Fig.4). Then, we may draw the conclusion that the slit-island method is one of the causes of the negative correlation between D_m and the toughness of materials.

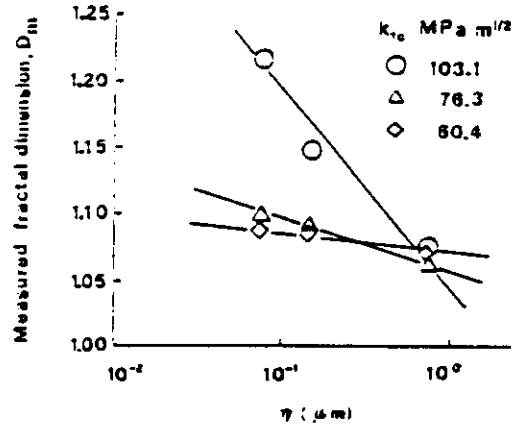


Fig.3 Measured fractal dimension D_m as a function of $\lg \eta$ on specimens with different K_{Ic} values.

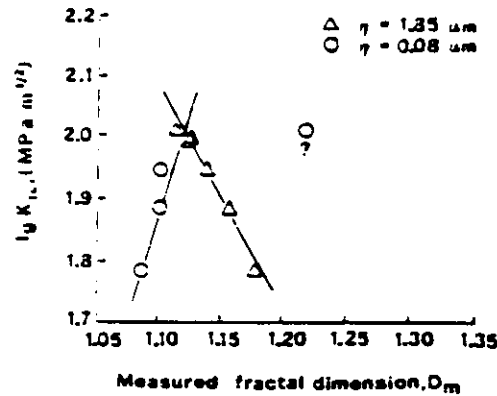


Fig.4 $\lg K_{Ic}$ as a function of measured fractal dimension D_m for two different η values.

We notice that

$$\alpha_0 = \frac{L_0(\eta)}{A_0^{1/2}(\eta)} \quad (D_F = 1).$$

From (8)

$$\begin{aligned} \alpha_n(\eta) &= \alpha_0 A_0(\eta)^{1/2} A_n(\eta)^{-1/2} \eta^{(1-D_F)/D_F} \\ &= \alpha_0 [A_0(\eta)/A_n(\eta)]^{1/2} \eta^{(1-D_F)/D_F} \end{aligned} \quad (9)$$

$A_0(\eta)/A_n(\eta)$ would approach a constant value as $n > n_c$ ($n_c \approx 20$ for a quadratic Koch island [8]; $n_c \approx 100$ for a triadic Koch island [9]) and then $\alpha_n(\eta)$ is size independent approximately. We obtain

$$D_m(\varepsilon)|_{\infty} \approx D_F. \quad (10)$$

Fractals in materials with only several self-similar generations ($n < n_c$) is not enough for measuring D_F with the slit-island method.

The condition that equation 10 holds is $n > n_c$; but the problem is how can we know our normalized yardstick length is small enough to have satisfied the condition. It is difficult to judge.

Furthermore, in many cases, the scaling range in materials is limited ($n < n_c$), and it is no use to reduce the yardstick length to the condition that $\varepsilon_m(n_m) < \varepsilon_c(n_c)$ because ε_m is out of the lower limit of the scaling range [9]. Sometimes, you obtain a positive correlation between D_F and K_{1c} (in brittle materials, η/L_0 is easy to be small). You still cannot judge if it is the real D_F of the fractured surfaces. You should check it by changing the yardstick in a certain range of scale to make sure that the measured value D_m does not change largely; then D_m is near the real D_F . It seems laborious. We think the best way to measure the fractal dimension of fractured surfaces may be the relations [2, 21, 22],

$$L_n(\eta) = L_0(\eta)^{D_F} \eta^{1-D_F} \quad (11)$$

We may measure the total length of crack propagation with different lengths of yardsticks. Then, D_F can be obtained by the slope of the linear relationship between $\log L_n(\eta)$ and $\log \eta$.

$$\log L_n(\eta) = D_F \log L_0(\eta) + (1 - D_F) \log \eta \quad (12)$$

$L_0(\eta)$ can also be determined after D_F is known. It seems hopeful to use the fractal dimension as a parameter for quantitative fractography.

VI. PHYSICAL SOURCES OF FRACTAL SURFACES

The fractal behaviour of a fractured surface is the total contributions of many elementary processes. Every elementary microstructure contributes its fractal or non-fractal behaviour at a certain range of scale (Fig. 1). Even in the same range, there are perhaps several elementary physical processes mix-up and lead to multifractality.

A log-log plot permits an analysis of the fractal character of a microstructural feature. This experimental microstructural analysis should be compared with the log-log plot of the fractured surface and then relates to the properties of materials. Unfortunately, little experimental data are available along this line at the moment.

Some theoretical models have been proposed for explanation of the relationship between fractal dimension and toughness of materials.

1. Intergranular fracture model [2]

Intergranular cracks may be connected to construct a Koch curve in a two-dimensional system [2, 23]. According to this model, G_{1c} (or K_{1c}) is enhanced.

$$G_{1c} = (G_{1c})_0 \varepsilon^{1-D_F} = (G_{1c})_0 (d/L_0)^{-0.26}$$

where, $D_F = 1.26$. It is calculated from geometrical consideration that " d " is the size of the grain, the lower limit for the scaling range and L_0 is a length related to the crack propagation, the upper bound for the scaling range, which can be determined by equation 11. The enhancement of G_{1c} (or K_{1c}) by self-similarity features of the fractured surface must not be very large. Enhancement by plastic deformation may be orders of magnitude higher [2, 20].

Similarly, a transgranular fracture model was proposed by Xie and Chen to predict their results of fractures in rocks [16].

2. Segment number effects [23, 9]

We suppose that new segments of microcracks of grain boundaries were superimposed on the preceding larger segment between large inclusions (Fig. 5).

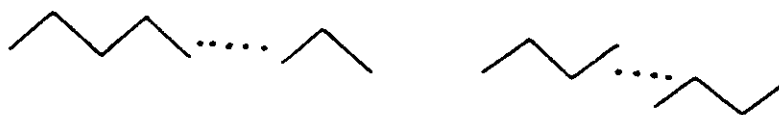


Fig. 5 Generators of fractal curves used to model the curves on a fractured surface: (a) N even; (b) N odd.

Then the fractal dimension may be

$$D_{0a} = \log N / \log [N \sin^2(\varphi/2)]^{1/2} 2 \sin^{-1}(1/N^{1/2}) < \varphi < \pi \quad (N = \text{even}) \quad (14)$$

$$D_{0b} = \log N / \log [1 + (N^2 - 1) \sin^2(\varphi/2)]^{1/2} \sin^{-1}[1/(N+1)^{1/2}] < \varphi < \pi \quad (N = \text{odd}) \quad (15)$$

Here, we have assumed the angles between two adjacent segments to be equal. We also know that the value of the angle φ depends on the grain configurations. In this case, the fractal dimension D_F may decrease with the increase of the segment number N .

This effect seems possible under the following condition and argument. High strength materials may induce much smaller cracks (inclusions) to propagate. This makes the crack propagation between two small inclusions easier. Then, the segment number N decreases and hence the fractal dimension increase. The correlation between D_F and K_{Ic} is therefore negative.

Ledge effects in crack propagation [24]

The vertical section method is employed to measure fractal dimensions of cross section profile of fractured surfaces of 30CrMnSiNi2A high strength steel under plane strain conditions. We found that the fractal dimensions of Koch curves along the direction of crack propagation, D_1 is different from that perpendicular to the direction of crack propagation, D_2 . A positive correlation between D_1 and K_{Ic} is obtained in comparison with a negative correlation between D_2 and K_{Ic} (Fig.6).

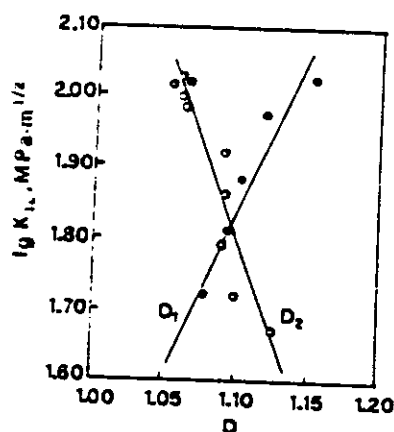


Fig.6 $\lg K_{Ic}$ vs fractal dimensions D_1 and D_2 .

However, the correlation between $(D_1 + D_2)$ (approximately equal to the fractal dimension of the fractured surface) and K_{Ic} is still a positive one (Fig.2).

Recently, Zhou and Thomson [25] pointed out that a ledge might be formed by passing a number of screw dislocations through the crack tip on a slip plane normal to the crack line. Ledges, a few atom spaces in height, will always emit dislocations before the crack will cleave, provided the angular orientation term is favourable. When a dislocation is emitted or ejected from the ledge crack, the ledge crack contains one less dislocation than before, and the ledge is one Burgers vector less in length. If we assume D_2 is a measure of the ledge height, D_2 may give some information on dislocation emission from the ledge cracks.

Changes in fracture mechanism [26]

Fractal dimension of different parts of a fractured surface of 30CrMnSiNi2A steel formed by slow crack propagation induced by the combining effect of hydrogen and static bending moment are determined by using the method of fracture profile analysis. The results showed that the fractal

dimension increases with increasing transgranular fracture relative to intergranular fracture as the crack propagate. This means that the increase of the fractal dimension responds to the increase of the energy needed to form the fracture surface and the process of forming a fractured surface by slow crack propagation is the one of increasing fractal dimension of the fractured surface; when the fractal dimension reaches a critical value, the crack propagation becomes unstable.

5. Fractal crack growth

Herrmann [3] described the fracture growth as a moving boundary problem similar to dielectric breakdown or viscous fingering. He modelled this problem on a square lattice by computer simulation and found that the patterns of cracks can be fractal even without including noise due only to the interplay of anisotropy and memory. The shapes of the cracks can be compared to the ones found experimentally for stress corrosion.

The important thing is that he assumed a beam model in which the p defined by

$$p = (f^2 + \tau \max(|m_1|, |m_2|))^\eta \quad (16)$$

where f is the traction force applied on the beam and m_1 and m_2 are the moments that are acting at the two ends of the beam; this p determines if the beam will be broken. Each time a beam is broken the shape of the crack and consequently the boundary conditions of the equation of motion changes and one has to discretized the equation again to know which beam to break next. If in equation 16 an exponential instead of a power law was used the structure seem to be dense. The form of equation 16 is empirical. For $\eta = 1$ this growth law is inspired by the von Mises yielding criterion, but it is not possible to derive it from first principles. The open problem is how can we find the relationship between equation 16 and many physical mechanisms of fracture, e.g. the above mentioned examples. Anyhow, he found some generic features due to mechanical instabilities leading to fracture. The specialities are in the form of equation 16 and the parameter of it. If a mechanism can be described as a power law it induces a fractal crack growth otherwise it does not.

Another interesting thing is that in his calculations the fractal dimension D_f depends on the parameter η . D_f decreases as η decreases. We know that the material fractures before yielding when $\eta < 1$. This result showed that low fractal dimension corresponds to brittle fractures. It seems reasonable.

VII. APPLICATIONS TO DEVELOPMENT OF NEW MATERIALS

Materials with fractal structures sometimes have bad properties; e.g. dendritic solidification in undercooled alloys may produce segregations of impurities and then lead to low toughness of materials.

Some properties may be enhanced by fractal structures. The enhancement of fracture toughness by fractal surfaces mentioned above is one example. Another example is that a fibre with fractal tree structure may increase the pull-out energy from the substrate (Fig. 7). The pull-out energy of a fibre with fractal tree structure from the brittle matrix has been calculated [27]. It is found that an increase of the number of generations may increase the efficiency of pull-out energy, $(W_{p0})_n / (W_{p0})$. The fractal tree of three generations with branched angles θ absorbs more energy than that of two generations with branched angle 2θ .

A model experiment has been done by Fu *et al.* [28]. The maximum pull-out stress and energy of a steel wire tree in resin was measured. Experimental data showed that the pull-out stress of a tree with one generation of branch angle 90° increases 75% of that of the single wire and a tree with two generations of branched angle 90° increases 160%. The pull-out energy of a fractal tree increases respectively. It seems possible to apply fractal structures to the development of high toughness materials.

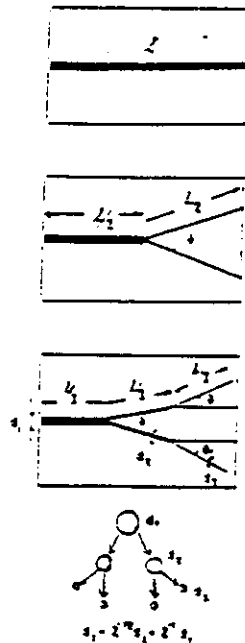


Fig.7a The fibre branches into two or three generations.

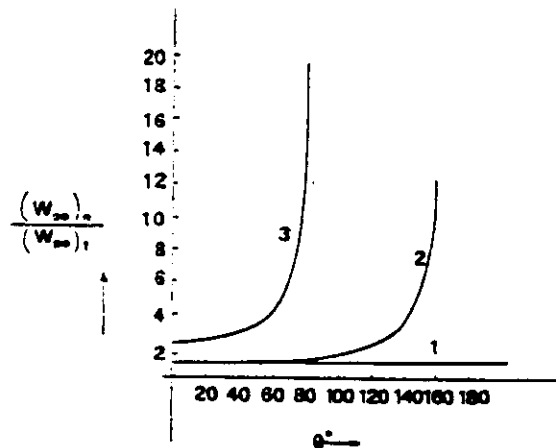


Fig.7b The relationship of the ratio $(W_{p0})_n / (W_{p0})_1$, with branched angles.

III. SUMMARY

1. Fractals in materials are more complicated than simple ideal models. Careful analyses are required for studies on fractured surfaces.
2. The relationship between fractal dimension of the fractured surfaces and the fracture toughness may be derived with fracture mechanics and has been verified by some experimental results. In general, the correlation between K_{Ic} and D_F is a positive one.
3. There are some difficulties for the use of the slit-island method to measure D_F . It is necessary to check the measured value by changing the yardstick length and to make sure it being yardstick length independent.
4. Fractal fractured surfaces may be formed by various physical sources. More experimental and theoretical studies are needed on this subject.
5. Applications to development of new materials are possible. This would draw our attention in the near future.

Acknowledgments

The author would like to thank Professor Abdus Salam, the International Atomic Energy Agency and UNESCO for hospitality at the International Centre for Theoretical Physics, Trieste. He would also like to thank Professor Stig Lundqvist for his encouragement on this direction of research in materials. This work was supported by the Science Fund Commission of China under the Grant No.5880056.

References

- 1) Mandelbrot B.B., Passoja D.E. and Paullay A.J.: Nature, 1984, 308, 721.
- 2) Lung C.W.: in Fractals in Physics, edited by Pietronero L. and Tosatti E., 1986, p.189, Elsevier, New York.
- 3) Herrmann H.J.: Physica A, 1990, 163, 359.
- 4) Mandelbrot B.B.: in Fractals, by Feder J., 1988, p.8, Plenum, New York.
- 5) Liu S.H.: in Proceedings of ICTP Working Party on Electrochemistry, Trieste, Italy, (August 17-September 7, 1990) to be published.
- 6) Tamás Vicsek, Fractal Growth Phenomena, 1989, pp.12-13, World Scientific, Singapore.
- 7) Hornbogen E.: International Materials Reviews, 1989, 34, 277.
- 8) Lung C.W. and Mu Z.Q.: Phys. Rev., 1988, 38 11781.
- 9) Lung C.W. and Zhang S.Z.: Physica D, 1989, 38, 242.
- 10) Mu Z.Q. and Lung C.W.: J. Phys. D: Appl. Phys., 1988, 21, 848.
- 11) Su H., Zhang Y.G. and Yan Z.Q.: Scripta Metall. Mater., 1991, 25, 651.
- 12) Mu Zaiqin, Li Shuqing and Lung C.W.: Materials Science Progress, 1990, 4, 247 (in Chinese).
- 13) Underwood E.E. and Banerji K.: Materials Engineering, 1986, 80, 1.
- 14) Pande C.S., Richards L.E., Louat N., Dempsey B.D. and Schwoeble A.J.: Acta Metallurgica, 1987, 35, 1633.
- 15) Richards L.E. and Dempsey B.D.: Scripta Metall., 1988, 22, 687.
- 16) Xie H.P. and Chen Z.D.: Acta Mechanica Sinica, 1988, 20, 264 (in Chinese).
- 17) Wang Z.G., Chen D.L., Jiang X.X., Ai S.H. and Sih C.H.: Scripta Metall., 1988, 22, 827.
- 18) Zhou X.Y., Chen D.L., Ke W., Zang Q.S. and Wang Z.G.: Materials Lett., 1989, 7, 473.
- 19) Wang X.W., Dong L.K. and Xiong L.Y.: J. Phys.: Condensed Matter, 1990, 2, 38.
- 20) Tzschichholz F. and Pfuff M.: Preprint for the Conference: "Fracture in Brittle Disordered Materials", 1991, Delft, The Netherlands.
- 21) Mandelbrot B.B., The Fractal Geometry of Nature, 1983, p.32, Freeman, San Francisco.
- 22) Feder J.: Fractals, 1988, Plenum, New York.
- 23) Zhang S.Z. and Lung C.W.: J. Phys. D: Appl. Phys., 1989, 22 790.
- 24) Mu Z.Q., Li S.Q. and Lung C.W.: Materials Science Progress, 1990, 4 247 (in Chinese).
- 25) Zhou S.J. and Thomson R.: J. Materials Research, 1991, (to be published).
- 26) Long Qiyi, Li Suqing and Lung C.W.: Materials Science Progress, 1990, 4, 241 (in Chinese).
- 27) Lung C.W.: preprint, ICTP, Trieste, No.IC/90/298, 1990.
- 28) Fu S.Y., Zhou B.L. and Lung C.W.: *Smart Mater. Struct.* 1 (1992) 180.

Multi-range Fractals in Materials

Qiwei LONG (C.W. Lung)

International Centre for Materials Physics, Institute of Metal Research, Academia Sinica, Shenyang 110015, China
[Manuscript received November 25, 1992]

A new model of multi-range fractals is proposed to explain the experimental results observed on the fractal dimensions of the fracture surfaces in materials. The relationship of multi-range fractals with multi-scaling fractals has been also discussed.

KEYWORDS: fractals, multi-range fractals, multi-scaling fractals, toughness

1. Introduction

Fractals in nature are different from rigorous models that the range of length in which self-similarity holds is bounded from above by the size of the fractal object and from below by the size of the smallest building block, and that they usually appear random but are similar in a statistical sense. Fractals in materials are much complicated. There are many objects which can form fractal structures, e.g. macroscopic crack lines or planes, vacancy clusters, dislocation lines, grain boundaries, dispersed particles etc. They are geometrically scaling in different ranges of scales [1,2].

Mandelbrot et al [3] showed that fractured surfaces are fractals in nature and that fractal dimensions of the surfaces correlate well with the toughness of the material. Along this line, the present author and collaborators did some experiments [4-8]. Experiments showed that in spite of the fractured surfaces are all inter-trans-granularly mixed character, an approximate constant value of fractal dimension in double logarithm plots was obtained in the range $2\ \mu\text{m} < \eta_i < 50\ \mu\text{m}$ [8]. On the other hand, two fractal dimensions were observed in one range of yardstick lengths [9]. This paper will propose a model of multi-range fractals to explain the reason why they are and discuss the relationship of multi-range fractals with multi-range fractals.

2. Two Fractals in a Range of Yardstick Lengths

The crack line is considered as Koch lines. For simplicity, we assume two fractals in a range of yardstick lengths. Two cases should be discussed.

2.1 Two fractals without overlap in the range of yardstick lengths (Fig.1)

Let $\varepsilon = \eta / L_0$; η and L_0 are the size of the smaller building block and the length of initiator respectively. ε is the relative length of the smaller building block normalized with L_0 . The ε_i is the normalized length of each of the smallest line segments. In Fig.1, we start to analyze the fractal structures from $\varepsilon_0 = 1$. The number of the smallest segments of the first fractal with dimension D_1 is

$$N(\varepsilon_1) = \varepsilon_1^{-D_1} \quad (1)$$

The second fractal with dimension D_2 starts from ε_1 ; the smallest segment of the first fractal is the length of the initiator of the second fractal. The total length of the two combined fractals may be expressed as follows:

$$\begin{aligned} L_1^T(\varepsilon_2) &= \varepsilon_1 N(\varepsilon_1) (\varepsilon_2 / \varepsilon_1)^{1-D_1} \\ &= \varepsilon_1^{1-D_1} (\varepsilon_2 / \varepsilon_1)^{1-D_1} \\ &= (\varepsilon_1 / \varepsilon_0)^{1-D_1} (\varepsilon_2 / \varepsilon_1)^{1-D_1} \quad (\varepsilon_0 = 1) \end{aligned} \quad (2)$$

The fracture toughness G_{IC}^0 or the critical crack extension force is enhanced by the fractal structures [4]. Then,

$$\begin{aligned} G_{IC}^F / G_{IC}^0 &= L_1^T(\varepsilon_2) \\ &= (\varepsilon_1 / \varepsilon_0)^{1-D_1} (\varepsilon_2 / \varepsilon_1)^{1-D_1} \end{aligned} \quad (3)$$

where, $G_{IC}^0 = 2\gamma_s \varepsilon_0$; the γ_s is the specific surface energy of the material.

For measurements of D_1 and D_2 , we may measure the total length $[L_1^T(\varepsilon)]$ of the crack line with different yardstick lengths (ε or η / L_0).

Invited paper presented at the 6th Workshop on Physics of Materials—Frontiers of Advanced Materials, Physics and Technology, 1992, Shenyang, China

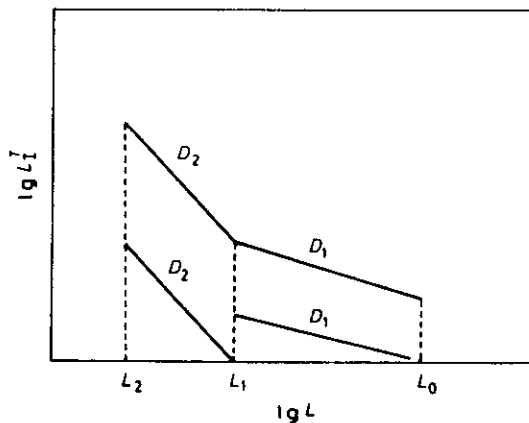


Fig. 1 Two fractals in different ranges of scale

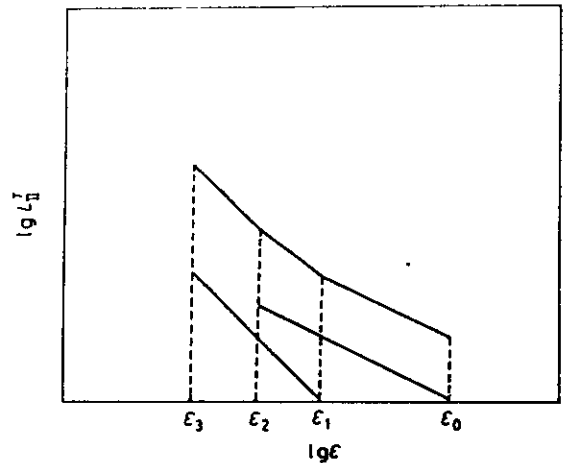


Fig. 2 Two fractals with overlap region of scale

Since

$$\lg L_1^T(\varepsilon) = (1-D_1)\lg \varepsilon \quad (\varepsilon_1 < \varepsilon < \varepsilon_0) \quad (4)$$

and

$$\begin{aligned} \lg L_1^T(\varepsilon) &= (1-D_1)\lg(\varepsilon_1/\varepsilon_0) + (1-D_2)\lg(\varepsilon/\varepsilon_0) \\ &= \text{const.} + (1-D_2)\lg \varepsilon \quad (\varepsilon_2 < \varepsilon < \varepsilon_1) \end{aligned} \quad (5)$$

D_1 or D_2 can be determined by measuring the slope of the straight line in $\lg L_1^T(\varepsilon)$ – $\lg \varepsilon$ plots in different ranges of yardstick lengths.

2.2 Two fractals with overlap in the range of yardstick lengths (Fig. 2)

We introduce a parameter α to express the width of the overlap range of yardstick lengths. Let

$$\varepsilon_1 = \varepsilon_0 / \alpha, \quad \varepsilon_2 = \alpha \varepsilon_3 \quad (6)$$

The width of the overlap, $\Delta \varepsilon$, can be expressed as follows,

$$\Delta \varepsilon = \varepsilon_1 - \varepsilon_2 = \varepsilon_0 / \alpha - \alpha \varepsilon_3 \quad (7)$$

When $\alpha = 1$, $\Delta \varepsilon = \varepsilon_0 - \varepsilon_3$, this is the case of two fractals overlapping each other in the whole range. When $\alpha = (\varepsilon_0 / \varepsilon_3)^{1/2}$, $\Delta \varepsilon = 0$, this is the case of two fractals without overlap. When $1 < \alpha < (\varepsilon_0 / \varepsilon_3)^{1/2}$, $0 < \Delta \varepsilon < \varepsilon_0 - \varepsilon_3$, the two fractals overlap each other partly.

If the smallest crack line segment is ε_3 , the total crack line length $L_{II}^T(\varepsilon_3)$ can be expressed as follows.

$$L_{II}^T(\varepsilon_3) = P_1 \varepsilon_2^{1-D_1} + (1-P_1) \alpha^{D_1-D_2} \varepsilon_3^{1-D_2} \quad (8)$$

where P_1 is the fraction of population of the first fractal.

The critical crack extension force is enhanced by the two fractals,

$$G_{IC}^F / G_{IC}^O = L_{II}^T(\varepsilon_3) \quad (9)$$

For measurements of D_1 and D_2 , we should use the following equations.

$$L_{II}^T(\varepsilon) = \varepsilon^{1-D_1} \quad (\varepsilon_1 < \varepsilon < \varepsilon_0) \quad (10-1)$$

$$\begin{aligned} L_{II}^T(\varepsilon) &= P_1 \varepsilon^{1-D_1} + (1-P_1) \alpha^{D_1-D_2} \varepsilon^{1-D_2} \\ & \quad (\varepsilon_2 < \varepsilon < \varepsilon_1) \end{aligned} \quad (10-2)$$

$$\begin{aligned} L_{II}^T(\varepsilon) &= P_1 \varepsilon_2^{1-D_1} + (1-P_1) \alpha^{D_1-D_2} \varepsilon^{1-D_2} \\ & \quad (\varepsilon_3 < \varepsilon < \varepsilon_2) \end{aligned} \quad (10-3)$$

Figure 3 shows the calculated curves for $\alpha = 1, 3$ and 5. In LONG's experiment [8], an approximate constant fractal dimension was obtained in spite of the fractured surfaces are all inter-transgranularly mixed character. This is the case of $\alpha = 1$. The calculated curve is approximately linear as the D_1 and D_2 differ not too large. In

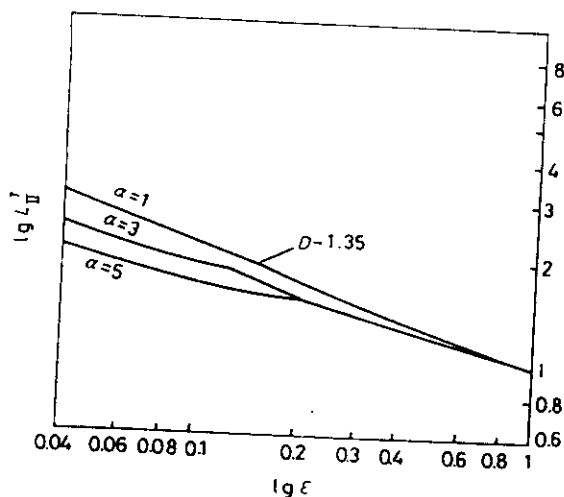


Fig.3 Calculated $\lg L_{II}^T - \lg \varepsilon$ curves for $\alpha = 1, 3$ and 5

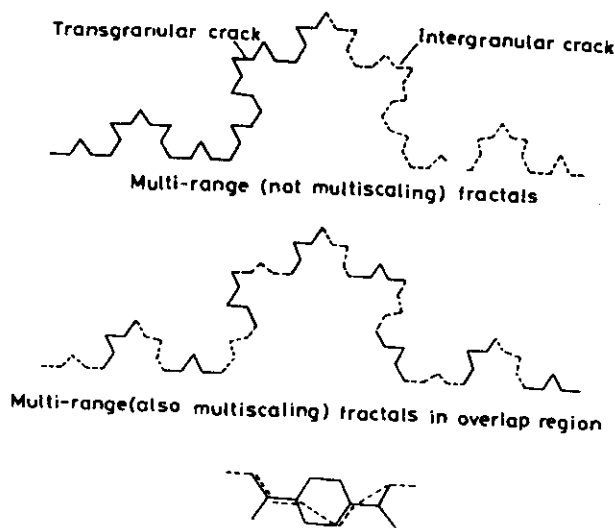


Fig.4 Multi-range fractals and multi-scaling fractals

MU's experiment [9], two fractal dimensions were observed. It seems to be the case of $\alpha = 5$ or 3 in which the two fractals never overlap or overlap partly.

We notice that Eq.(10-3) is not so simple as Eqs.(10-1), (4) and (5).

$$L_{II}^T(\varepsilon) = A + B\varepsilon^{1-D_2} \quad (\varepsilon_3 < \varepsilon < \varepsilon_2) \quad (11)$$

In this case, we introduce a parameter for de-

termination of D_2 ,

$$Y_{II}^T(\varepsilon) = L_{II}^T(\varepsilon) - A \quad (12)$$

then,

$$Y(\varepsilon) = B\varepsilon^{1-D_2} \quad (13)$$

$$\lg Y(\varepsilon) = \text{const.} + (1-D_2)\lg \varepsilon \quad (14)$$

D_2 can only be determined by the slope of the line in $\lg Y(\varepsilon) - \lg \varepsilon$ relationship figure. However, usually experimentalists draw $\lg L_{II}^T(\varepsilon) - \lg \varepsilon$ figure. It would be wrong, because

$$\lg L_{II}^T(\varepsilon) \neq \text{const.} + (1-D_2)\lg \varepsilon!$$

To determine both the values of D_1 and D_2 in the overlap region is not so easy. We should use Eq.(10-2). However, it is possible to solve it numerically.

3. Multi-scaling Fractals in Multi-range Fractals

In fractures, multi-range fractals even with overlap regions are not necessary multi-scaling fractals. If G_{IC}^T (transgranular) differs greatly from G_{IC}^I (intergranular), the transgranular crack and intergranular crack would not mix. At lower stress level, the grain boundaries break at first. When the stress raises to a high value, transgranular cracking follows. Each kind of crack has its own self-similar system. They only superpose in the material (Fig.4). However, if G_{IC}^T is near G_{IC}^I , the probability of intergranular cracking is near the same as the transgranular one, these two processes may mix and form one multi-scaling self-similar fractal system.

In our case, the physical quantity which we want to measure is the fracture toughness of the complex system. In fracture mechanical analysis, it is equal to two times the specific surface energy multiplied by the crack surface area; or the length of crack line in 2-D fracture mechanical problem. The fraction of the total physical measure includes two factors, i.e. the probability of intergranular cracking, $P_o = G_{IC}^T / (G_{IC}^I + G_{IC}^T)$ and the length of the segment. According to Feder [10] and assuming parameters from LONG's experiment [8], the spectrum of fractal dimensions, $D(q)$ for the multi-fractal measure of G_{IC}^T / G_{IC}^I on a geometrical set $D(0) = 1$ (a straight line) can be obtained [11].

Up till now, we only discussed the case of two fractals. Expressions for N fractals can be found in Ref.[11].

4. Summary

(1) Unlike the original theoretical model of fractals with infinite number of generations, fractals in nature are bounded from above by the size of the initiator and from below by the size of the smallest building block. There are a number of multi-range fractals existing in materials. In order to study the relationship between fractal structure and property, we should make sure which fractal structure is in relation to the property at first.

(2) Multi-range fractals with overlap regions in the range of yardstick lengths are not necessary to be multi-scaling fractals. However, only if the probabilities of different physical mechanisms are nearly same, processes may mix and form one multi-scaling self-similar fractal system.

(3) The concept of multi-range fractals would be possible extended to other processes; e.g., the fractal cluster growth, surface dynamics and etc.

Acknowledgement

This work was supported by the National Natural Sci-

ence Foundation of China

REFERENCES

- (1) E.Hornbogen: *Int. Mater. Rev.*, 1989, **34**, 277.
- (2) C.W.Lung: *Nonlinear Phenomena in Materials Science*, Vol.2, eds., G.Martin and L.Kubin, 1992, 483.
- (3) B.B.Mandelbrot, D.E.Passoja and A.J.Paullay: *Nature*, 1984, **308**, 721.
- (4) C.W.Lung: *Fractals in Physics*, ed. by L.Pietronero and E.Tosatti, Elsevier, New York, 1986, 189.
- (5) C.W.Lung and Z.Q.Mu: *Phys. Rev. B.*, 1988, **38**, 11781.
- (6) C.W.Lung and S.Z.Zhang: *Physica D.*, 1989, **38**, 242.
- (7) Z.Q.Mu and C.W.Lung: *J. Phys. D: Appl. Phys.*, 1988, **21**, 848.
- (8) Q.Y.Long, Suqing Li and C.W.Lung: *J. Phys. D: Appl. Phys.*, 1991, **24**, 602.
- (9) C.W.Lung and Z.Q.Mu: *Scientia Sinica*, 1993 (to be published)
- (10) J.Feder: *Fractals*, Plenum Press, 1988, 81.
- (11) C.W.Lung: in *Proc. Int. Workshop on Statistical Physics*, Beijing Normal University Press, 1993 (to be published)